IJE TRANSACTIONS B: Applications Vol. 39, No. 08, (August 2026) 1878-1892

International Journal of Engineering

Journal Homepage: www.ije.ir

A Modified Impedance-Based Loss of Field Detection Method of Synchronous Generator in the Presence of Series Capacitor and its Over-voltage Devices

H. Yaghobi*

Faculty of Electrical and Computer Engineering, Semnan University, Semnan, Iran

PAPER INFO

Paper history:
Received 30 June 2025
Received in revised form 08 September 2025
Accepted 26 September 2025

Keywords:
Synchronous Generator
Series Capacitor
Loss of Field Relay
Over-voltage Devices

ABSTRACT

Loss of field (LOF) detection of synchronous generators in power networks compensated with series capacitors (SCs) create challenging conditions. Fault currents passing through the capacitors can generate over-voltages that exceed the SC ratings, necessitating protection by Metal Oxide Varistors (MOVs). However, when the MOV and capacitor are part of the fault impedance loop, unfavorable conditions arise for LOF relays, including current and voltage fluctuations, high-frequency oscillations from MOVs, and sub-harmonic oscillations. Therefore, this work presents a new modified impedance-based function for LOF protection in the presence of a series capacitor and its over-voltage devices. An analytical solution is proposed to correct the impacts of SCs on LOF protection, which has not been documented previously. The non-linear behavior of the varistor in parallel with the series capacitor is approximated using a linear series R-X impedance model. The operation of the modified LOF function is considered with various capacitor placements, and power network variations such as compensation levels and load changes under complete and partial LOF scenarios. Simulations conducted in MATLAB/Simulink demonstrate the effectiveness and reliability of the proposed method, highlighting its independence from the power system structure while addressing existing relay challenges.

doi: *10.5829/ije.2026.39.08b.09*

Graphical Abstract

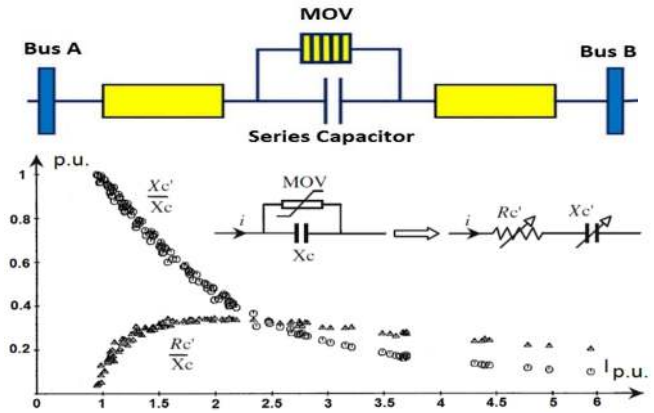

$$R_c' = X_c(0.0745 + 0.49e^{-0.243I_{pu}} - 35e^{-5I_{pu}} - 0.6e^{-1.4I_{pu}})$$

$$X_c' = X_c(0.1010 - 0.0057I_{pu} + 2.088e^{-0.8566I_{pu}})$$

$$\Downarrow$$

$$\vec{Z}_{LOF\ Relay} = \frac{\vec{Z}_G + \vec{Z}_T + \vec{Z}_{SYS} + R_c' - jX'}{(1 - m\,e^{-j\varphi})} - \vec{Z}_G$$

*Corresponding author email: yaghobi@semnan.ac.ir (H. Yaghobi)

Please cite this article as: Yaghobi H. A Modified Impedance-Based Loss of Field Detection Method of Synchronous Generator in the Presence of Series Capacitor and its Over-voltage Devices. International Journal of Engineering, Transactions B: Applications. 2026;39(08):1878-92.

NOMENCLATURE

X_e	System external reactance	δ, w, w_s	Rotor angle, rotor speed and synchronous speed
R_v	Voltage-transformer (VT) ratio	V_d, I_d	The d-axis components of V and I
R_c	Current-transformer (CT) ratio	V_q, I_q	The q-axis components of V and I
Kv, MVA	Machine's rated voltage and power	X_d, X_q	The d-axis and q-axis synchronous reactances
V_S	Machine terminal voltage	X'_d, X'_q	The d-axis and q-axis transient reactances
Z_G, Z_T	Generator and transformer impedance	X''_d, X''_q	The d-axis and q-axis sub-transient reactances
Z_{SYS}	Lumped system impedance	X_{ad}	The d-axis mutual reactance
X_C	Series compensation capacitor reactance	T'_{do}, T''_{do}	The d-axis transient and sub-transient open circuit time constants
i, v	Resistor current and voltage	T'_{qo}, T''_{qo}	The q-axis transient and sub-transient open circuit time constants
β , $I_{p.u.}$	Constant and normalized current	R_f, X_f	Rotor winding resistance and reactance
I_{pr} , I_c	Capacitor current of the protective level and the capacitor fault current	R_a, X_{ls}	Stator winding resistance and leakage reactance
m, k	Series capacitor locations and degrees of compensation	ψ_d, ψ_q	The d-axis and q-axis stator flux linkages
VG	Generator excitation voltage	ψ_{fd}, ψ_{d1}	The d-axis field and damper flux linkages
p_e, p_m	Active and mechanical power of the generator	ψ_{1q}, ψ_{2q}	The q-axis dampers flux linkages
V , I , φ	Voltage and current of the stator and their phase angle difference	V_f, I_f	Field voltage and field current
H	The total inertia constant of the generator	Z_c, R'_c, X'_c	Linear equivalent and series R-X impedance of the parallel arrangement of MOV and series capacitor

1. INTRODUCTION

Series compensation on long transmission lines is growing and unavoidable for various reasons, such as improving the power system stability, increasing voltage control, and transmission power (1, 2). On the other hand, installing series capacitors (SCs) in transmission lines makes the protection more complicated. The amount of this difficulty depends on the installation location and the size of the capacitor. The higher size of the series compensation makes the protection more difficult. The installation place and the technique of series capacitor bypass are also very significant in the protective strategy (3, 4). When the series capacitor and its bypass system are located in the fault impedance loop, the conditions for the LOF relay become unfavorable. The relay computes the impedance value utilizing the voltage and current at the generator station. With the operation of the capacitor bank and its MOV, the currents and voltages of the power network change. Consequently, the impedance calculated by the LOF function is adversely affected. As stated above, the LOF relay is a distance type (5, 6) and it should be mentioned that the performance of distance relays for different faults with the existence of FACTS devices has been considered in many publications. It is worth highlighting that the effects of FACTS devices on the distance relay are different from the effects of the LOF distance function and should be investigated, separately. Consequently, some research works evaluated the impacts of FACTS devices on the LOF distance relay (7-9). In this regard, a wavelet-based scheme for LOF protection in the presence of STATCOM have been presented by Dolatabadi et al. (10). In this work, LOE detection and its differentiation from other network disturbances are discussed and the importance of intelligent signal processing approaches in modern FACTS-equipped networks is emphasized. Hasani et al. (11) presented a complete review of current LOF protection strategies for synchronous generator. This work highlights emerging trends such as digital signal processing methods and adaptive techniques that increase the accuracy and speed of detection.

Furthermore, some papers have been announced specifically on the effect of series capacitors on line distance function relays. As an example, adaptive distance protections in transmission lines compensated with series capacitors have been presented based on different techniques. The method presented by Ghassemi et al. (12) used the voltage compensation for calculating the voltage drop on the series capacitors and modifying the relay settings. Another adaptive technique using impedance estimation considering MOV operation, power system condition, and fault resistance in series compensated lines is proposed by Biswal et al. (13). Also, a scheme using residual current in distance function relays for series compensated lines is suggested by Ghassemi and Johns (14). Some other methods based on artificial intelligence for distance function relays in series

compensated lines have been proposed by several research scientists (15-21). Furthermore, neural network intelligent algorithm and data mining method are proposed by Rahmkhoda et al. (22, 23) and Silva et al. (24) to enhance the safety of the LOE protection of synchronous generator in the presence of unified power flow controller and SVC. Supervised learning algorithms to distinguish LOF from power swings, was proposed by Gulati and Verma (25). They demonstrated the ability of artificial intelligence to recognize complex dynamic behaviors. Furthermore, a machine learning ensemble framework for detecting LOF conditions have been presented by Ramadoss and Muthiah (26). In this research, several models are presented to improve classification accuracy and reduce false detection rate. However, these methods need a lot of training. On the other hand, in the previous study of the author, only the performance of two LOF relays with positive and negative offset has been compared with the presence of the series capacitor, and no solution has been provided (27).

Therefore, in this paper, the impact of SCs and their over-voltage devices on the LOF relay has been carefully analyzed. This research describes a modified impedance-based function for LOF protection of generators in the power networks with fixed series compensation. The parallel arrangement of the nonlinear resistance and series capacitor is approximated by the linear series impedance R-X. In other words, an analytical method is developed considering MOV operation, different series capacitor locations, and variations in the power network such as different degrees of compensation, load, and different LOF scenarios. In summary, the important points in the literature review of this article can be found as follows:

- The LOF relay is basically a distance type because it uses the voltage and current at the relay location to make a decision.
- The problems of distance relays, including transmission line distance relays and generator field relays in the existence of FACTS devices, have been investigated in several articles. In these articles, usually no solution is presented and only the problems are investigated or mostly solutions based on artificial intelligence are presented to solve the issues. However, these methods need a lot of training data for different conditions of the network.
- The problems of transmission line distance relays in the existence of series compensation capacitors, have been investigated in some papers. In these papers, similar to the previous case, most solutions based on artificial intelligence are presented to solve the problems. However as mentioned above, these approaches require a lot of training data for different conditions of the power system.
- The impacts of the series capacitor on the LOF protection of the synchronous generator have not been evaluated in the literature or at least no solution has been presented for it.

Therefore, the key contributions of this study are as follows:

- The effect of the series capacitor on the LOF protection of the synchronous generators is investigated and an analytical solution for its correction is presented which has not been reported in the literature yet.
- This analytical technique is developed taking into account MOV operation, different capacitor locations, and variations in the power network such as degrees of compensation, load, and different LOF conditions including complete and partial LOF scenarios.
- The parallel arrangement of a highly non-linear varistor and series capacitor is estimated by a linear series R-X impedance.
- Based on the point that these kinds of relays are currently operative in loss of field protection of synchronous generators, therefore, it has been tried to solve some of the issues of these kinds of relays.

The LOF relay considered in this research is the Berdy distance function and the “Matlab/Simulink” software has been used for time domain simulation of the SCs and their over-voltage devices. Extensive results indicate the effectiveness and satisfactory performance of the suggested method. The rest of this article is organized as follows: Section 2 explains the modified impedance-based LOF protection of a generator in the presence of a series capacitor and its over-voltage devices. In section 3, the performances of the proposed technique are presented and the results are analyzed. Finally, section 4 concludes the investigation.

2. MODIFIED LOF PROTECTION IN THE SERIES COMPENSATED LINE

Coordination between LOF protection with generator under-excited capability (GUEC) limit, steady-state stability limit (SSSL), and generator under-excitation limiter (UEL) is very important issue. The salient-pole generator capability limits are illustrated in Figure 1. This machine has minor end core area losses. Consequently, the GUEC limit has been represented by the current limit of the stator winding (i.e. arc from B to D). It is worth mentioning that the leading VAR limit of the GUEC is determined by the portion of the arc from C to D. Furthermore, during the normal mode of operation of the generator, the SSSL shows how far the machine can operate under-excited area of the capability curve (9, 28, 29).

In fact, in coordination studies, the SSSL is utilized to adjust the machine UEL. The SSSL characteristic is drawn in Figure 1, as portion of a circle with the following center and radius.

$$Center = 0,\ \frac{V_s^2}{2}\left(\frac{1}{X_e}-\frac{1}{X_d}\right),\ Radius = \frac{V_s^2}{2}\left(\frac{1}{X_e}+\frac{1}{X_d}\right) \quad (1)$$

where X_e is the system external reactance, X_d is d-axis steady-state machine reactance and V_s is the machine terminal voltage.

In addition to these, the machine UEL is set to prevent the reduction of the excitation over the heating limit of the stator-end region. Usually, this characteristic is set to 80–85% of one of the SSSL characteristic or the GUEC characteristic with minimum time delay (9). In order to coordinate the three characteristics GUEC, SSSL, and UEL to LOF relay, these three characteristics should be converted in the R-X plane (9) (see Figure 2(a)). In this figure, R_v is the voltage-transformer (VT) ratio, R_c is the current-transformer (CT) ratio, kV is the machine's rated voltage and MVA is the machine's rated power.

On the other hand, it should be mentioned that the common technique to detect the LOF in a generator is to use a relay introduced by Berdy (30) as presented in Figure 2(b). This relay has two operation zones with a negative offset equal to $x'_d/2$. The diameter of the first zone is one p.u. (machine base) and the diameter of the second zone is xd. In this relay, typically, 0.1s time delay is considered for the first zone and, 0.5 to 0.6 s time delay is considered for the second zone. These intentional time delays prevent relay misoperation during stable power swings and transient conditions (31-33). It should be noted that transient stability studies should be conducted to see if the above time delays are sufficient to prevent inadvertent tripping during stable power swings and transient conditions. However, usually for simplicity these time delays are typically considered.

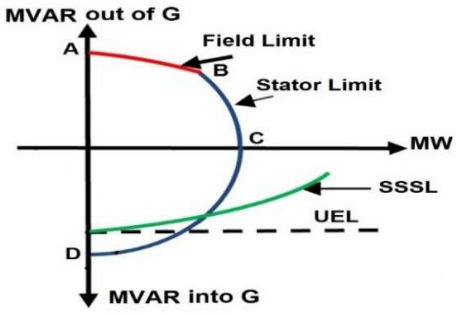

Figure 1. Capability limits of a generator

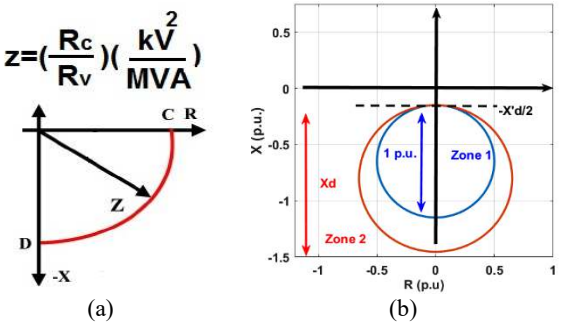

(a) (b)

Figure 2. Synchronous generators characteristic (a) GUEC, SSSL, and UEL in the R-X plane (b) Berdy LOF characteristic and impedance locus at the generator terminal following LOF and stable power swing condition

2. 1. Distance Relay Problem due to Compensation

The series capacitor and its protective devices against overvoltage, despite the advantages in the power network, cause problems for protection relays such as sub-harmonic oscillation, current and voltage changes, and additional transients (4). Following the occurrence of the fault, impedance-based relays in series compensated networks face various challenges, and changes in current and voltage data occur. Depending on the location of the fault and the compensation degree, the impedance-based relay may experience a fundamental frequency resonant situation with high voltage and current values. One of these impedance-based relays is the Berdy LOF relay. The impedance trajectory measured at location of the relay is affected by voltage changes caused by the series capacitors after the fault.

2. 2. Modified Impedance-Based LOF Protection

In this research, it is assumed that the LOF condition occurred simultaneously during the three-phase short circuit fault. Figure 3 shows approximated equivalent circuit for research on the detection of LOF condition during fault in a compensated power network with a MOV-protected series capacitor. This situation activates MOV. In fact, when the capacitor and its MOV are located in the fault impedance loop, the conditions for the LOF relay at the generator location become unfavorable.

In this network, V_S is machine terminal voltage, Z_G, Z_T, Z_{SYS}, X_C, and Z_C are generator impedance, transformer impedance, lumped system impedance, series compensation capacitor reactance, and linear equivalent impedance of the parallel arrangement of MOV and series capacitor, respectively. The generator terminal voltage can be calculated as follows:

$$V_S = \sqrt{V_d^2 + V_q^2} \quad (2)$$

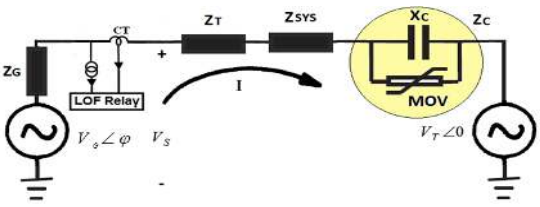

Figure 3. Configuration of the network studied

In this investigation, the complete model of the synchronous generator is used. This model takes into account all the basic aspects of the behavior of the synchronous generator, including its electrical and mechanical characteristics. In fact, this complete model provides the possibility of simulation and detailed analysis of the performance of the synchronous generator in different operating conditions. A three-phase salient pole synchronous generator with one field winding (subscripted by *f)*, has been used. A lumped winding (subscripted by 1d) was used to consider the impact of the induced currents in the rotor core.

On the other hand, two fabricated lumped windings (subscripted by *1q* and *2q*) were used to consider the effects of damper bars in the rotor. It should be noted that in this work eight equations have been used to model the performance of a three-phase salient pole synchronous generator, including two mechanical Equations, 3 and 4, and six electrical equations in *dq* form, Equations 3 to 8 (34).

$$\frac{2H}{w_s}\frac{dw}{dt} = p_m - p_e \tag{3}$$

$$\frac{d\delta}{dt} = w - w_s \tag{4}$$

$$\frac{1}{w_s}\frac{d\psi_d}{dt} = V_d + w\,\psi_q + R_a I_d \tag{5}$$

$$\frac{1}{w_s}\frac{d\psi_q}{dt} = V_q - w\,\psi_d + R_a I_q \tag{6}$$

$$T'_{do}\frac{dE'_q}{dt} = -E'_q - (X_d - X'_d)[I_d - \frac{X'_d - X''_d}{(X'_d - X_{ls})^2}(\psi_{1d} + (X'_d - X_{ls})I_d - E'_q] + E_f \tag{7}$$

$$T''_{do}\frac{d\psi_{1d}}{dt} = -\psi_{1d} + E'_q - (X'_d - X_{ls})I_d \tag{8}$$

$$T'_{qo}\frac{dE'_d}{dt} = -E'_d + (X_q - X'_q)[I_q - \frac{X'_q - X''_q}{(X'_q - X_{ls})^2}(\psi_{2q} + (X'_q - X_{ls})I_q + E'_d] \tag{9}$$

$$T''_{qo}\frac{d\psi_{2q}}{dt} = -\psi_{2q} - E'_d - (X'_q - X_{ls})I_q \tag{10}$$

where

$$E'_q = \frac{X_{ad}}{X_{ff}}\psi_{fd},\ E'_d = -\frac{X_{aq}}{X_{11q}}\psi_{1q},\ E_f = \frac{X_{ad}}{R_f}\psi_{1q}V_f \tag{11}$$

Also, the variables of the machine can be calculated as:

$$\psi_d = -X''_d\,I_d + \frac{X''_d - X_{ls}}{X'_d - X_{ls}}E'_q + \frac{X'_d - X''_d}{X'_d - X_{ls}}\psi_{1d} \tag{12}$$

$$\psi_q = -X''_q\,I_q + \frac{X''_q - X_{ls}}{X'_q - X_{ls}}E'_d + \frac{X'_q - X''_q}{X'_q - X_{ls}}\psi_{2q} \tag{13}$$

This model of three-phase salient pole generator is simulated in Matlab/Simulink software. Furthermore, standard models of ESDC1A and IEEEG1 have been utilized to model the machine excitation system and governor, respectively (35). The detailed data of these models are given in Appendix (see Tables 2 and 3). In the network, illustrated in Figure 3 the LOF relay impedance measured at the machine terminal can be determined as follows:

$$\vec{Z}_{\text{Relay}} = \frac{\vec{V}_S}{\vec{I}} = \frac{(\vec{V}_G - Z_G\vec{I})}{\vec{I}} = \frac{V_G\angle\varphi}{\vec{I}} - \vec{Z}_G \tag{14}$$

where

$$\vec{I} = \frac{\vec{V}_G - \vec{V}_T}{Z} = \frac{V_G\angle\varphi - V_T\angle 0}{\vec{Z}_G + \vec{Z}_T + \vec{Z}_{SYS} + \vec{Z}_C} \tag{15}$$

On the other hand:

$$\frac{\vec{V}_T}{\vec{V}_G} = \frac{|V_T|\angle 0}{|V_G|\angle\varphi} = \frac{|V_T|}{|V_G|}e^{-j\varphi},\ m = \frac{|V_T|}{|V_G|} \tag{16}$$

Therefore:

$$\vec{V}_T = (\vec{V}_G)\,m\,e^{-j\varphi} \tag{17}$$

By substituting Equation 17 into Equation 15, the $\vec{I}$ can be written as:

$$\vec{I} = \frac{\vec{V}_G(1 - m\,e^{-j\varphi})}{\vec{Z}_G + \vec{Z}_T + \vec{Z}_{SYS} + \vec{Z}_C} \tag{18}$$

Finally, by applying Equation 18 to Equation 14, the impedance seen by the LOF relay can be calculated as:

$$\vec{Z}_{\text{Relay}} = \frac{\vec{Z}_G + \vec{Z}_T + \vec{Z}_{SYS} + \vec{Z}_C}{(1 - m e^{-j\varphi})} - \vec{Z}_G \tag{19}$$

As stated earlier, Z_c is the equivalent impedance of the parallel arrangement of MOV and series capacitor which is fully described in the following. Series capacitor banks are constructed by combining parallel and series units to obtain the desired nominal values. Also, these capacitor banks are designed in such a way that rated current values are obtained. Series capacitor banks are exposed to severe stress during fault situations. Fault current passing through the capacitor bank produces voltages that exceed the rated amount of the capacitor. Hence, in modern capacitor banks, Metal Oxide varistors (MOVs) as shown in Figure 4(a) are usually used to protect against over-

voltages (4). In addition, the capacitor block illustrated in Figure 4(a) contains a "damping device" that is a current-limiting circuit. A typical non-linear voltage-current characteristic (4) of this surge arrester called a varistor, is illustrated in Figure 4(b).

When the voltage reaches its limit, a large amount of current passes through the varistor, and the voltage through the series compensation capacitor is limited. The voltage-current characteristic of this surge arrester can be approximated as follows:

$$v = ki^{\beta} \tag{20}$$

where i is resistor current, β is a constant smaller than one and v is resistor voltage. Equation 20 can be written as:

$$\alpha = \ln v = \ln k + \beta \ln i \;\Rightarrow\; v = e^{\alpha} = e^{(\ln k + \beta \ln i)} \tag{21}$$

By substituting Equation 18 into Equation 21, the MOV voltage can be written as:

$$v = e^{(\ln k + \beta \ln(\frac{\vec{V}_G(1-me^{-j\varphi})}{\vec{Z}_G + \vec{Z}_T + \vec{Z}_{SYS} + \vec{Z}_C}))} \tag{22}$$

It should be noted that during a complete LOF V_G is zero. However, in partial LOF, V_G is not zero and its amount is a percentage of the machine's complete field voltage (i.e. less than 100 %). Using the experimental data, a fundamental frequency model of the non-linear MOV has been remodeled to a series R-X model (36). This is shown in Figure 5, that R_c' and X_c' are controlled by the instantaneous current (36). It can be seen that capacitive reactance and resistance are non-linear, and are functions of the normalized current $I_{p.u.}$.

In other words, the parallel arrangement of non-linear varistor and series compensation capacitor can be modeled by a linear series R-X impedance as illustrated in Figure 5. Using the data from Figure 5 and least-squares curve fitting, this linear model can be found as follows (36, 37):

$$\begin{aligned} R_c' &= X_c(0.0745 + 0.49e^{-0.243I_{pu}} - 35e^{-5I_{pu}} - 0.6e^{-1.4I_{pu}}) \\ X_c' &= X_c(0.1010 - 0.0057I_{pu} + 2.088e^{-0.8566I_{pu}}) \end{aligned} \tag{23}$$

where X_c is nominal capacitor reactance, $I_{p.u.}=I_c/I_{pr}$ (the current is normalized), I_{pr} is the capacitor current of the protective level and I_c is the capacitor fault current.

It should be noted that the value of the capacitor fault current should be determined and sent to the relay location in the generator terminal through a communication channel.

Specific data of the series compensation module that is required in this method is given in Appendix (see Table 2).

In power system relaying, the acceptable latency and required bandwidth for a data communication channel can vary significantly based on the specific application, the type of relay being used, and the overall system requirements. It is worth noting that the impedance LOF relay is a slow relay. Hence, there is no need for a very high-speed communication channel to transmit capacitor's fault current value to the generator's terminal. However, the acceptable latency for protection relays in the range of 1 to 10 milliseconds is suitable for the proposed method. On the other hand, the bandwidth requirement for proposed relay is low since the method send small amounts of critical data (i.e. the capacitor's fault current value) at high rates. Typical bandwidth requirements are around 10 to 100 kbps.

Furthermore, since relay 78 (out-of-step relay) is a backup for relay 40 (LOF relay), the generator will not be left unprotected in the event of a failure or cyber-attack on this data communication channel (Please see the answer to your comment 3.).

Another point to consider is that whenever a fault occurs, there is a DC component in the fault current. To remove the DC offset, various methods mentioned by Yaghobi (38) can be used. However, it should be noted that in this research assumes that the DC offset has been removed first.

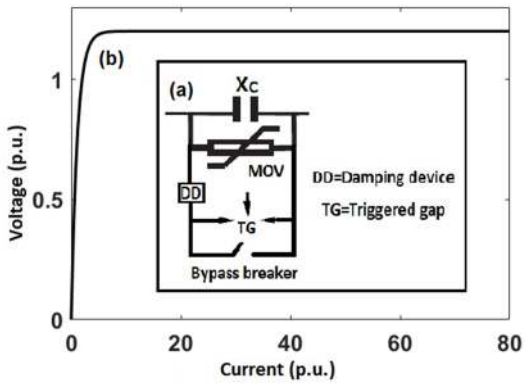

Figure 4. Series capacitor (a) Used model (b) Voltage-current characteristic of the MOV.

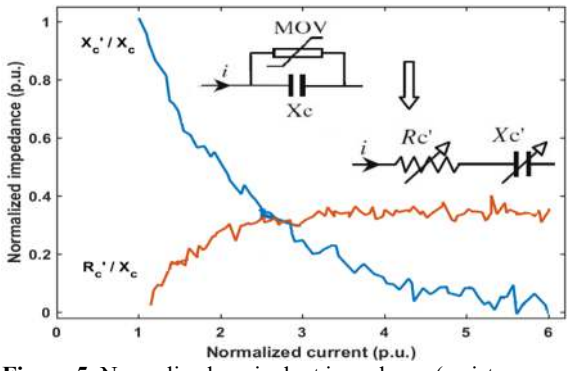

Figure 5. Normalized equivalent impedance (resistance and reactance) versus normalized current of the series compensation capacitor and its MOV protection

The typical value of I_{pr} is 2-2.5 times of the full load current. It should be noted that R_c' and X_c' is normalized by dividing by X_c and precise amounts of R_c' and X_c' depends on the amplitude of the fault current passing through the MOV (varistor). Rahmkhoda et al. (23) determined the equivalent impedance; only the values of X_c and I_{pr} should be determined. The normalized value of R_c' and X_c' versus $I_{p.u.}$ is plotted in Figure 5. These values change with the current and reach almost zero as $I_{p.u.}$ is increased more than 6 p.u. According to Rahmkhoda et al. (23) and data from Figure 5, the linear equivalent impedance of the MOV-protected series compensation capacitor can be found as follows (36, 37):

$$Z_c(I_{p.u.}) = \begin{cases} -jX_c & if \ \ I_{p.u.} < 0.98 \\ R_c' - jX_c' & if \ \ I_{p.u.} \geq 0.98 \end{cases} \quad (24)$$

It is worth highlighting that if the capacitor current is more than 98% of the protective level current, the MOV conducts. However, below this value, the MOV does not act and is out of service. In other words, if the protective voltage level of the series compensation capacitor exceeds its threshold value under fault conditions, the MOV will conduct and as a result, the impedance of the series capacitor/MOV combination will vary.

3. PERFORMANCES OF THE PROPOSED TECHNIQUE

The operation of the modified LOF function is evaluated in the presence of a series capacitor at different locations for a 400 kV power system as illustrated in Figure 3. In the transmission line, every phase of the series compensation module includes the series compensation capacitor and the capacitor is protected by a MOV. In the protection of a synchronous generator with the series compensated line, the series capacitor location and degrees of compensation are important. Therefore, this research has been done for various series capacitor locations (i.e. m = 0, m = 0.5, m = 1), for varying degrees of compensation (i.e. k = 0.4, k = 0.7), and for different LOF conditions including complete and partial LOF scenarios (i.e. VG = 0 p.u. and VG = 0.5 p.u.). Furthermore, four critical loading points of the machine are considered in this research (i.e. light and heavy loading with the lagging and leading power factor conditions).

3. 1. Performances of the LOF Relay without Coordination with other Characteristics

The results for the conventional and proposed technique are provided in Table 1 for various system situations. As stated earlier, adding series compensation capacitors in the transmission line complicates the protection of the generator, and the degree of this complexity changes with the degree of compensation and the installation location of the capacitors along the transmission line. In other words, in transmission lines compensated with series capacitors, observable characteristics may change significantly and this problem may cause difficulties for conventional LOF relaying schemes. The voltage, current, and impedance measured by the relay have significant changes depending on the size and installation location of the series capacitor.

For a clear demonstration, the machine output voltage and current following LOF under inductive heavy load condition (L1 = 0.9 + j0.3 p.u.) is shown in Figure 6(a). LOF condition in this case occurs after 10 s of starting the simulation time. As it is displayed in Figure 6(a), the generator output voltage decreases to a negative value during this situation. In addition, with the existence of a series compensation capacitor, the rate of reduction of the machine terminal voltage is reduced, which makes the LOF condition to be detected later. The output current of the generator is also presented in this figure. As shown in this figure, the existence of a series capacitor causes the machine armature to remain longer under the fault current conditions and its amount increases to a consideration value. Furthermore, Figure 6(b) presents the machine output active and reactive power under inductive heavy load condition (L1 = 0.9 + j0.3 p.u.).

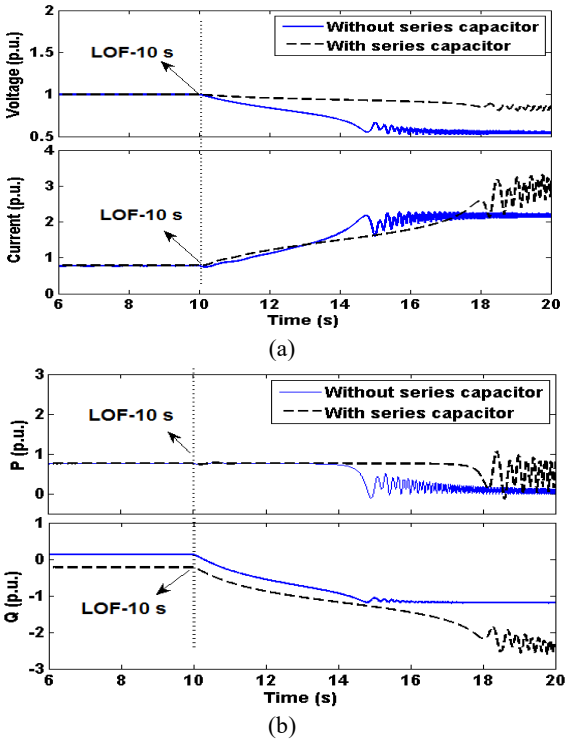

Figure 6. The generator output following LOF under inductive heavy load condition (L1 = 0.9 + j0.3 p.u.) (a) Terminal voltage and current (b) Active and reactive power

As can be seen from this figure, similar to the terminal voltage, next the happening of the LOF condition, the machine output reactive power decreases to a considerable negative value, while the output active power has an almost constant value before loss of synchronism. The effect of the partial LOF on the machine output under the capacitive heavy load condition (L3 = 0.7 -j0.5 p.u.) is shown in Figure 7. The PLOF condition in this case occurs after 10 s of starting the simulation time. In PLOF condition, the rotor field of the generator is partially lost, while in complete LOF, the rotor field of the machine is completely lost. The comparison between Figures 6 and 7 denote that the impact of the partial LOF on the generator output is less intense than a complete LOF.

In PLOF condition, depending on the amount of residual excitation voltage, the rate of voltage drop and the reactive power of the machine terminal are reduced compared to the complete LOF. Therefore, the operation time of the relay increases. In PLOF conditions, because the excitation voltage of the generator is not completely lost, the machine absorbs less reactive power from the grid than a complete LOF condition. The lower percentage of field is lost, the generator loses synchronism at a longer time, which means the relay will have more time to detect, however this detection will be more difficult. Therefore, the worst case for the conventional relay is a low percentage of PLOF under loading with the leading power factor condition, which

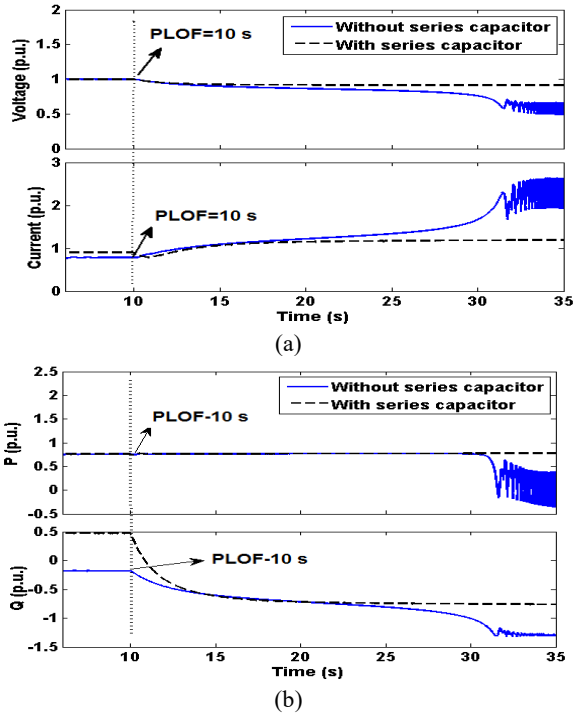

Figure 7. The generator output following PLOF under capacitive heavy load condition (L3 = 0.7 -j0.5 p.u.) (a) Terminal voltage and current (b) Active and reactive power

greatly increases the relay operation time or in some cases, the relay does not operate. Long-term reactive power drain may cause tripping of the line relays and general power network instability. This situation becomes worse with the presence of a series capacitor. Because some of the reactive power required by the generator in this condition is supplied by the series capacitor.

If the series capacitor is placed in the middle of the transmission line, its effectiveness is increased, especially for very long transmission lines. When the capacitor is installed in the middle of the transmission line, the changes in the variables (i.e. voltage, current, and impedance) are less than when the capacitor is located at the beginning or end of the line. Therefore, according to Table 1, in general, the time to detect the LOF conditions by the relay when the series capacitor is installed in the middle of the line is less than the other two cases. It should be mentioned that the relay operating time is higher under a capacitive load condition than an inductive load condition. In addition, the relay operation time increases in the partial LOF condition compared to the complete LOF condition. Therefore, as stated earlier, the worst case for the relay is partial LOF under capacitive load condition, which greatly increases the relay operation time. Furthermore, when the series capacitor is in service, generator protection becomes more complicated, and this condition can potentially cause the relay not to operate.

Accordingly, it can be seen from the simulation results presented in Table 1, that the presence of a series capacitor under PLOF (VG =0.5 p.u.) with capacitive load conditions causes the conventional LOF relay not to work during cases 3, 9, 15, 27, and 33. In other words, during these cases, the conventional LOF relay does not issue a trip signal whereas the modified technique trips at 4.15 s (5.65-1.5), 4.02 s (5.52-1.5), 3.93 s (5.43-1.5), 4.43 s (5.93-1.5), and 4.21 s (5.71-1.5) for cases 4, 10, 16, 28, and 34, respectively. The partial LOF condition in all cases occurs after 1.5 s of starting the simulation time. In other cases, the presence of the series capacitor causes the conventional relay to take a longer tripping time compared with the suggested modified technique. In fact, the modified technique has effectively reduced the tripping time associated with the presence of the series compensation capacitor. It should be noted that the amount of equivalent impedance of the compensation capacitor and its MOV (Z_c) in simulation has been presented in Table 1. Figure 8(a) presents the impedance trajectory calculated by the modified and conventional LOF function following LOF (i.e. VG = 0 p.u.) during cases 7, and 8 under inductive heavy load condition (i.e. L1=0.9+j0.3 p.u.) with the presence of series capacitor and its over-voltage devices. In these cases, the series compensation capacitor is considered at the beginning of the transmission line with 70% compensation (i.e. m=0, k=0.7). Both impedance locus enters into the operating

zone of the relay. However, the conventional technique trips at 2.32 s (3.82–1.5) which has been reduced to 2.01 s (3.51–1.5) by the modified technique.

Moreover, to illustrate the similarity in characteristics, Figure 8(b) illustrates the impedance loci computed by the modified and conventional LOF function following complete LOF during cases 25, and 26 under inductive heavy load condition (i.e. L1 = 0.9+j0.3 p.u.) with the presence of series capacitor and its over-voltage devices. In these cases, the series compensation capacitor is considered at the end of the transmission line with 40% compensation (i.e. m=1, k=0.4). Both impedance locus enter into the operating zone of the relay. However, the conventional technique trips at 3.68 s (5.18–1.5) which has been reduced to 2.82 s (4.32–1.5) by the modified technique. As reported in Table 1 and according to Figures 8(a) and 8(b), it can be clearly seen that these two techniques are robust adequate to correctly distinguish the complete LOF situation under inductive loading with the presence of a series capacitor and its over-voltage devices.

In other words, there is no significant difficulty. However, only the conventional relay needs more time to send a trip signal compared to the modified technique. Additionally, the performance of the modified and conventional function under LOF (VG =0 p.u.) with the heavy capacitive loading conditions (i.e. L3 = 0.7-j0.5 p.u.) in the presence of series capacitor and its over-voltage devices are shown in Figures 8(c), 8(d), and 8(e). In cases 13 and 14 (see Figure 8(c)) the series compensation capacitor is considered at the middle of the transmission line with 40% compensation (i.e., m=0.5, k=0.4). Also, in cases 19 and 20 (see Figure 8(d)), the series compensation capacitor is considered at the middle of the transmission line, but with 70% compensation (i.e., m=0.5, k=0.7). In cases 25 and 26 (see Figure 8(e)), the series compensation capacitor is considered at the end of the transmission line with 40% compensation (i.e., m=1, k=0.4). As reported in Table 1 and according to Figures 8(c), 8(d), and 8(e), it can be clearly seen that these two techniques are robust adequate to correctly distinguish the complete LOF condition with the presence of a series capacitor and its over-voltage devices. However, the conventional relay takes a longer time to send a trip signal compared to the modified technique. It should also be noted that this trip time is longer than the inductive loading with similar conditions. The conventional technique trips at 2.44 s (3.94-1.5), 2.14 s (3.64-1.5), and 4.372 s (5.872-1.5) for cases 13, 19, and 25, respectively whereas the modified technique trips at 1.77 s (3.27-1.5), 1.62 s (3.12-1.5), and 3.22 s (4.72-1.5) for cases 14, 20, and 26, respectively. It can be obviously realized that in all cases the trip time of the modified technique has been effectively reduced compared to the conventional relay. On the other hand, as mentioned before, the worst case of relay operation is partial LOF under capacitive load conditions. Therefore, the performance of the modified and conventional function under PLOF (VG =0.5 p.u.) with the heavy capacitive loading condition (i.e. L3 = 0.7 -j0.5 p.u.) in the presence of series capacitor and its over-voltage devices are shown in Figures 8(f) and 8(g). In cases 9 and 10 (see Figure 8(f)), the series compensation capacitor is considered at the beginning of the transmission line with 70% compensation (i.e. m=0, k=0.7).

Furthermore, in cases 15 and 16 (see Figure 8(g)), the compensation capacitor is considered at the middle of the transmission line with 40% compensation (i.e. m=0.5, k=0.4). At these conditions, the conventional LOF relay does not operate for cases 9 and 15 whereas the modified technique trips at 4.02 s (5.52-1.5) and 3.93 s (5.43-1.5) for cases 10 and 16, respectively. In the following, in cases 9, 10, 21, and 22, it is supposed the generator operates at the light capacitive loading conditions with partial LOF event. The impedance loci computed by the conventional and the modified function after PLOF with the light capacitive loading conditions (i.e. L4 = 0.1-j0.1 p.u.) in the presence of series compensation capacitor and its over-voltage devices are also shown in Figures 9(h) and 9(k).

In cases 9 and 10 (see Figure 9(h)) the compensation capacitor is considered at the beginning of the transmission line with 70% compensation (i.e. m=0, k=0.7). Moreover, in cases 21 and 22 (see Figure 9(k)), the compensation capacitor is considered at the middle of the transmission line with 70% compensation (i.e. m=0.5, k=0.7). In all cases, the impedance locus enters into the operating zone of the relay. The conventional technique trips at 4.12 s (5.62-1.5), and 3.64 s (5.14-1.5) for cases 9, and 21, respectively whereas the modified technique trips at 2.84 s (4.34-1.5), and 2.78 s (4.28-1.5) for cases 10, and 22, respectively. It can be realized that in all cases the trip time of the modified technique has been effectively reduced compared to the conventional relay.

Furthermore, other percentages of PLOE under capacitive load conditions were examined and it was determined that the proposed method has performed successfully up to V_G=0.75 (i.e. 25 percent of excitation has been lost). The proposed method has had unsuccessful performance under conditions where V_G is greater than 0.75 in several cases (V_G>0.75). These results are also presented in Table 1.

3. 2. Performances of the LOF Relay in Coordination with GUEC, SSSL, and UEL Characteristics As stated earlier, coordination between LOF protection with GUEC, SSSL, and UEL is very important issue and special attention should be paid for relay operation under partial LOF during capacitive load conditions. In this regard, a significant problem that must be considered during this

TABLE 1. Performance of modified and conventional LOF function in the presence of series capacitor and its over-voltage devices

Case	Capacitor location	Degree of Compensation	$Z_C(\Omega)$	Mode of LOF	Protection method	Type of loading (p.u.)			
						Lagging		Leading	
						L1- Heavy 0.9+j0.3	L2- Light 0.1+j0.2	L3- Heavy 0.7-j0.5	L4- Light 0.1-j0.1
						Detection time (s)			
1	m=0	k= 0.4	$R'_c=8.18$ $X'_c=3.42$	V_G=0	Conventional	4.13	3.52	4.35	3.71
2					Proposed	3.54	3.32	3.8	3.5
3				V_G=0.5	Conventional	5.62	5.42	×	6.35
4					Proposed	4.81	4.38	5.65	4.58
5				V_G=0.75	Conventional	6.74	6.44	×	7.58
6					Proposed	5.72	5.25	6.67	5.47
7		k= 0.7	$R'_c=20$ $X'_c=12.41$	V_G=0	Conventional	3.82	3.5	3.95	3.7
8					Proposed	3.51	3.14	3.61	3.52
9				V_G=0.5	Conventional	5.2	4.85	×	5.62
10					Proposed	4.56	4.12	5.52	4.34
11				V_G=0.75	Conventional	6.24	5.78	×	6.74
12					Proposed	5.46	4.91	6.54	5.208
13	m=0.5	k= 0.4	$R'_c=7$ $X'_c=2.78$	V_G=0	Conventional	3.65	2.8	3.94	3.22
14					Proposed	3.14	2.62	3.27	2.95
15				V_G=0.5	Conventional	5.4	5.22	×	6.12
16					Proposed	4.66	4.12	5.43	4.52
17				V_G=0.75	Conventional	6.46	6.26	×	×
18					Proposed	5.48	4.98	6.32	5.29
19		k= 0.7	$R'_c=12.26$ $X'_c=4.87$	V_G=0	Conventional	3.41	2.98	3.64	3.01
20					Proposed	3.04	2.72	3.12	2.82
21				V_G=0.5	Conventional	4.95	4.62	5.73	5.14
22					Proposed	4.45	4.10	5.25	4.28
23				V_G=0.75	Conventional	5.94	5.49	×	×
24					Proposed	5.34	4.89	6.3	5.01
25	m=1	k= 0.4	$R'_c=6.07$ $X'_c=2.36$	V_G=0	Conventional	5.18	4.12	5.872	4.65
26					Proposed	4.32	3.95	4.72	4.05
27				V_G=0.5	Conventional	5.62	5.18	×	6.63
28					Proposed	4.52	4.12	5.93	4.69
29				V_G=0.75	Conventional	6.74	6.28	×	×
30					Proposed	5.44	4.93	7.104	5.6
31		k= 0.7	$R'_c=10.62$ $X'_c=4.12$	V_G=0	Conventional	4.38	3.87	4.82	4.05
32					Proposed	3.65	3.01	3.91	3.62
33				V_G=0.5	Conventional	4.89	4.7	×	5.85
34					Proposed	3.75	3.62	5.71	4.51
35				V_G=0.75	Conventional	5.85	5.61	×	×
36					Proposed	4.53	4.39	6.91	5.43

coordination is the presence of series capacitor and its over-voltage devices. Figure 9(a) shows a sample case study, in which the voltage reduces about 14%. In this case, the impedance locus of the modified LOF function does not penetrate the reduced zone of the relay characteristic (coordinated with GUEC, SSSL, and UEL characteristics). Therefore, non-LOF condition is detected. However, it enters the zones 1 and 2 with original setting (i.e. Z_{1old} and Z_{2old}) and the LOF relay with original setting misoperates in this condition. Such a voltage reduction will be alarmed by undervoltage (UV) supervising element. It should be noted that usually the UV relay is set at 80%–90% of rated voltage of the machine to pick up with a time delay of 0.25–1 s. In this study, the UV relay is set at 87% of the rated voltage of the machine with a time delay of 1s. Figure 9(b) shows the generator terminal voltage during undervoltage condition (i.e. related to Figure 9(a)). As a result of the undervoltage condition, generator terminal voltage begins to reduction and falls below the UV threshold at which it picks-up at 6 seconds after the start of the simulation and assigning a one second time delay. On the other hand, in order to investigate the security of the proposed modified LOF function, stable power swing condition as another non-LOF event has been evaluated in this section. It should be mentioned that there are various types of unstable power swing or out-of-step (OOS) relays, some of which are presented by Yaghobi (39). These relays are different from LOF relays. Therefore, this article does not discuss the distinction and diagnosis of OOS and LOF from each other and only the distinction of LOF from stable power swings is examined. In fact, the impedance-based LOF protections are prone to mal-operation under stable power swing conditions and the LOF relay must be blocked during the stable power swings to avoid misoperation. These methods overcome this possible mal-operation by assigning a time delay.

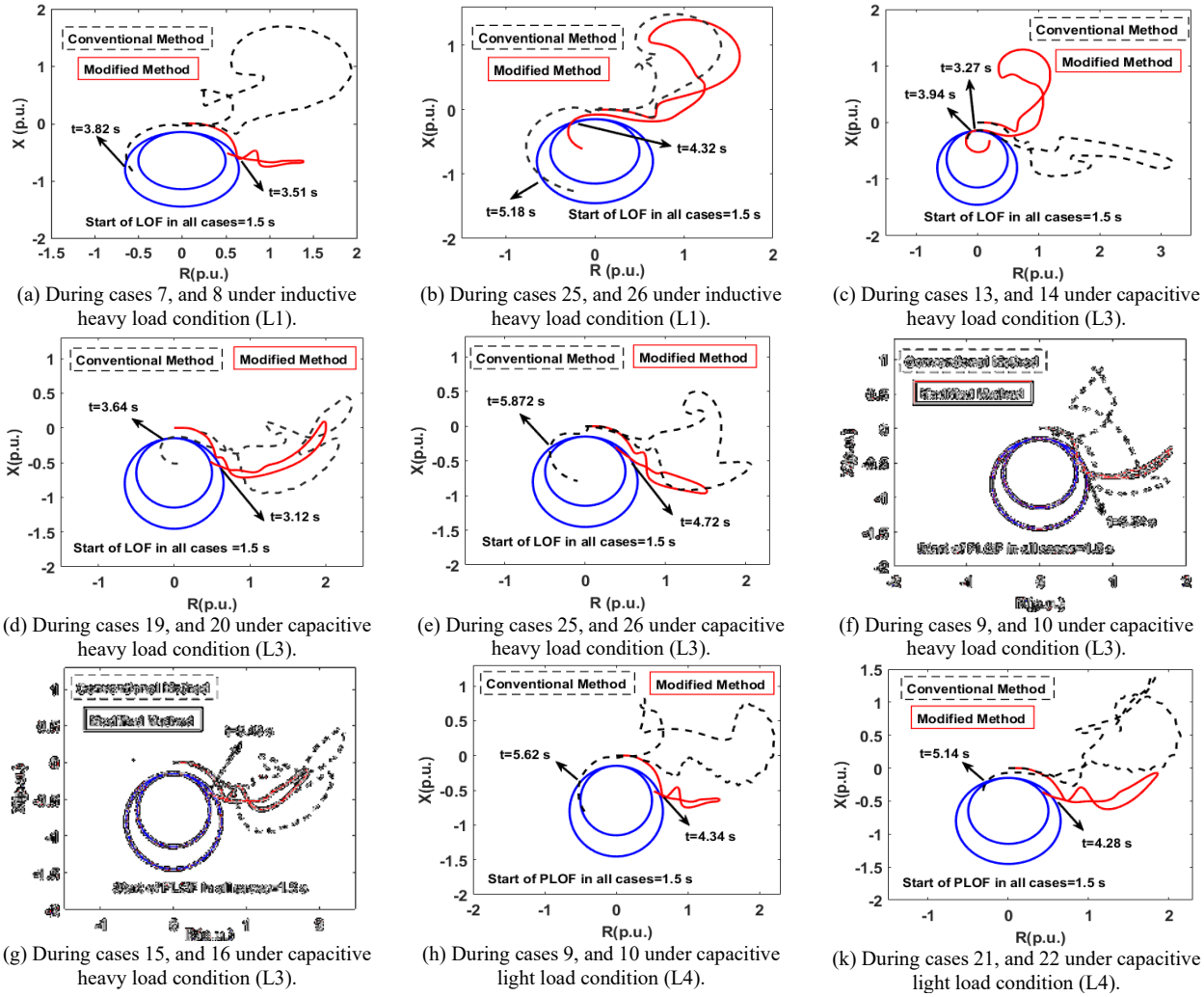

(a) During cases 7, and 8 under inductive heavy load condition (L1).

(b) During cases 25, and 26 under inductive heavy load condition (L1).

(c) During cases 13, and 14 under capacitive heavy load condition (L3).

(d) During cases 19, and 20 under capacitive heavy load condition (L3).

(e) During cases 25, and 26 under capacitive heavy load condition (L3).

(f) During cases 9, and 10 under capacitive heavy load condition (L3).

(g) During cases 15, and 16 under capacitive heavy load condition (L3).

(h) During cases 9, and 10 under capacitive light load condition (L4).

(k) During cases 21, and 22 under capacitive light load condition (L4).

Figure 8. Calculated impedance trajectory by the modified and conventional LOF function for LOF and PLOF event

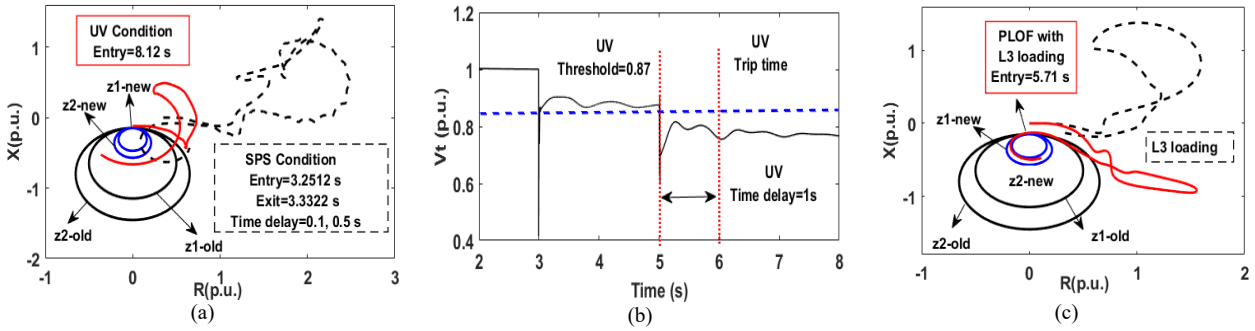

Figure 9. (a) Performances of the LOF Relay in coordination with GUEC, SSSL and UEL characteristics under stable power swing and voltage reduction condition (b) Generator terminal voltage and undervoltage (UV) element trip signal associated with Figure 9 (a) (c) Performances of the LOF Relay in coordination with GUEC, SSSL and UEL characteristics under capacitive heavy load condition (L3) in the absence and presence of the PLOF (VG =0.5 p.u.)

Figure 9(a) also shows the impedance locus measured by modified LOF function in the presence of series capacitor and its over-voltage devices under stable power swing condition. This condition has been created by applying a three-phase short circuit fault at the generator terminal for time for the duration of 12 cycles (0.2 s). It can be seen that in this condition the impedance trajectory of the modified LOF function enters into the reduced zone of the relay characteristic in 3.2512 s and leaves it after 0.081 s.

As stated in section II, in LOF relay, 0.1 s time delay is considered for the first zone and, 0.5 to 0.6 s time delay is considered for the second zone. These intentional time delays should be utilized to ride over the transient situations that might cause misoperation during transient and stable power swings. Therefore, the mentioned time delays are sufficient to prevent the relay misoperation in this case. Therefore, non-LOF condition is detected and the modified LOF function is robust enough. In another case studies, the performances of the modified function under the heavy capacitive loading condition (i.e. L3 = 0.7 -j0.5 p.u.) in the absence and presence of the PLOF (VG =0.5 p.u.) condition are shown in Figure 9(c). With the absence of the PLOF condition, the impedance locus of the modified LOF function does not penetrate the reduced zone of the relay characteristic. Therefore, non-LOF condition is detected. However, with the existence of the PLOF condition, the impedance trajectory of the modified LOF function enters into the reduced zone of the relay characteristic (coordinated with GUEC, SSSL, and UEL characteristics). Therefore, PLOF condition is detected and modified technique trips at 4.21 s (5.71-1.5). In fact, the modified function remains secure under this condition.

3. 3. Switching Effect of the Capacitor on the Performances of the LOF Relay

Transient condition due to the switching of the capacitor, is one of the most important issues that have been investigated in this study. As stated in section II, in LOF relay, 0.1 s time delay is considered for the first zone and, 0.5 to 0.6 s time delay is considered for the second zone. These intentional time delays should be utilized to ride over the transient situations that might cause misoperation during transient and stable power swings. The value of this time delay should be equal to the minimum time needed to ride over transient situations. Consequently, allocating an deliberate time delay is commonly used to ride over the probable misoperation of the LOF relay (30-33). The bypass breaker removes or inserts the capacitor bank into the circuit (see Figure 4(a)).

This breaker provides protection for imbalances or failures. When the triggered gap or bypass breaker operates, this function creates a transient condition whose frequency depends on the capacitance and inductance of the circuit. This frequency is generally in the range of 300 to 1000 Hz (0.001 s to 0.0033 s). Consequently, according to the above discussion, a time delay of 0.1 seconds for the first zone and 0.5 to 0.6 seconds for the second zone is enough to overcome this type of transient. On the other hand, the frequency of transient waves produced by the switching of power circuit breakers is typically in the range of kilohertz (kHz) to megahertz (MHz) (40).

These transient waves are usually caused by abrupt variations in current and voltage due to switching or connecting and disconnecting the loads. Therefore, in this case, similar to the previous case, a time delay of 0.1 seconds for the first zone and 0.5 to 0.6 seconds for the second zone is enough to ride over these transient situations. For instance, Figure 10 shows a typical behavior of the impedance trajectory calculated by the modified LOF function following a transient condition. In this case, the impedance trajectory enters into the reduced zone of the relay characteristic in 4.4511 s and leaves it after 0.0022 s. Therefore, the mentioned time delays are sufficient to prevent the relay misoperation.

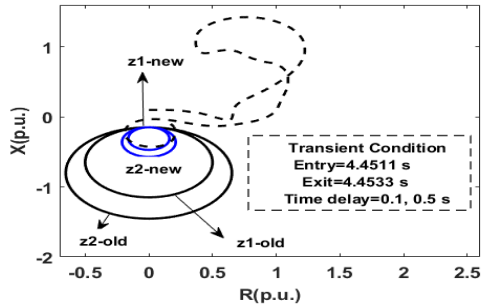

Figure 10. Performances of the LOF Relay in coordination with GUEC, SSSL and UEL characteristics under transient condition due to the switching of the capacitor

4. CONCLUSION

The installation of compensation capacitors in electrical networks is on the rise, both in terms of the number of installations and their capacity, due to their numerous advantages. However, while impedance-based distance relays are effective for detecting LOF conditions, the presence of compensation capacitors and their associated over-voltage devices can hinder the operation of conventional LOF relays. Specifically, series capacitors protected by Metal Oxide Varistors (MOVs) create challenging conditions for impedance-based LOF relays that rely on traditional impedance calculation methods. To enhance the security of these relays, it is crucial to account for the influence of series capacitors and their over-voltage devices. This research introduces a new adaptive relay setting technique that addresses these challenges. The technique incorporates an analytical solution to correct the effects of series capacitors on LOF protection for synchronous generators, a topic not previously documented in the literature. This analytical method takes into consideration MOV operation, various capacitor locations, and fluctuations within the power network, including degrees of compensation, load variations, and different LOF scenarios such as complete and partial LOF. Additionally, the parallel configuration of highly non-linear varistors with series capacitors is approximated using a linear series R-X impedance model. Given that these types of relays are currently employed for loss of field protection in synchronous generators, this research aims to resolve some of the existing issues associated with them. Simulation results across various scenarios demonstrate the effectiveness and satisfactory performance of the proposed modified technique, which remains independent of the power system's structure.

5. ACKNOWLEDGMENT

This research is funded by Semnan University, research grant No @ 140386.

6. REFERENCES

1. Yaghobi H. Precision enhancement of the traditional sub-synchronous analysis by using frequency components of instantaneous magnetic flux. IET Generation, Transmission & Distribution. 2021;15(22):3100-14. https://doi.org/10.1049/gtd2.12243
2. Abbasi M, Shayestehkhah H, Tousi B. Application of an additive self-tuning controller for static synchronous series compensator for damping of sub-synchronous resonance oscillations. International Journal of Engineering, Transactions B: Applications. 2018;31(4):564-73. https://doi.org/10.5829/ije.2018.31.04a.07
3. Firouzjah KG. Fault location on compensated transmission lines without current measurement. International Journal of Engineering, Transactions C: Aspects. 2018;31(12):2044-51. https://doi.org/10.5829/ije.2018.31.12c.08
4. Anderson PM, Henville CF, Rifaat R, Johnson B, Meliopoulos S. Power system protection: John Wiley & Sons; 2021.
5. Yaghobi H, Mortazavi H, Ansari K, Rajabi Mashhadi H, Khorashadzadeh H, Borzoe H, editors. A novel flux-based method for synchronous generator loss of excitation protection. 25th International Power System Conference, PSC2010, Nov. 2010, Tehran, Iran. 2010. https://civilica.com/doc/133208/
6. Haseli MR, Haghjoo F, Hasani A. A new air gap flux-based technique to detect loss of field in synchronous generators. IET Electric power applications. 2024;18(5):543-55. https://doi.org/10.1049/elp2.12410
7. Yaghobi H. A new adaptive impedance-based LOE protection of synchronous generator in the presence of STATCOM. IEEE Transactions on Power Delivery. 2017;32(6):2489-99. https://doi.org/10.1109/TPWRD.2017.2647746
8. Ghorbani A, Soleymani S, Mozafari B. A PMU-based LOE protection of synchronous generator in the presence of GIPFC. IEEE Transactions on power delivery. 2015;31(2):551-8. https://doi.org/ 10.1109/TPWRD.2015.2440314
9. Elsamahy M, Faried SO, Sidhu T. Impact of midpoint STATCOM on generator loss of excitation protection. IEEE Transactions on power delivery. 2013;29(2):724-32. https://doi.org/ 10.1109/TPWRD.2013.2281581
10. Dolatabadi S, Seyedi H, Tohidi S. A new method for loss of excitation protection of synchronous generators in the presence of static synchronous compensator based on the discrete wavelet transform. Electric Power Systems Research. 2022;209:107981. https://doi.org/10.1016/j.epsr.2022.107981
11. Hasani A, Liang X, Sanaye-Pasand M, Abedini M, Haghjoo F, Bak CL. Loss of Field Protection for Synchronous Generators: Current Practice and Future Trends. IEEE Transactions on Industry Applications. 2025. https://doi: 10.1109/TIA.2025.3573992
12. Ghassemi F, Goodarzi J, Johns A, editors. Method for eliminating the effect of MOV operation on digital distance relays when used in series compensated lines. The 1997 32 nd Universities Power Engineering Conference, UPEC'97 Part 1(of 2); 1997.
13. Biswal M, Pati BB, Pradhan AK. Adaptive distance relay setting for series compensated line. International Journal of Electrical Power & Energy Systems. 2013;52:198-206. https://doi.org/10.1016/j.ijepes.2013.03.018
14. Ghassemi F, Johns A. Investigation of alternative residual current compensation for improving series compensated line distance protection. IEEE transactions on power delivery. 2002;5(2):567-74. https://doi.org/ 10.1109/61.53058
15. Bachmann B, Novosel D, Hart D, Hu Y, Saha MM, editors. Application of artificial neural networks for series compensated

line protection. Proceedings of International Conference on Intelligent System Application to Power Systems; 1996: IEEE.

16. Fahim SR, Sarker SK, Muyeen S, Sheikh MRI, Das SK, Simoes M. A robust self-attentive capsule network for fault diagnosis of series-compensated transmission line. IEEE Transactions on Power Delivery. 2021;36(6):3846-57. https://doi.org/10.1109/TPWRD.2021.3049861
17. Taheri MM, Seyedi H, Nojavan M, Khoshbouy M, Ivatloo BM. High-speed decision tree based series-compensated transmission lines protection using differential phase angle of superimposed current. IEEE Transactions on Power Delivery. 2018;33(6):3130-8. https://doi.org/10.1109/TPWRD.2018.2861841
18. Parikh UB, Das B, Maheshwari RP. Combined wavelet-SVM technique for fault zone detection in a series compensated transmission line. IEEE Transactions on Power Delivery. 2008;23(4):1789-94. https://doi.org/10.1109/TPWRD.2008.919395
19. Ebadi A, Hosseini S, Abdoos A. A new restricted earth fault relay based on artificial intelligence. International Journal of Engineering, Transactions A: Basics. 2019;32(1):62-70. https://doi.org/10.5829/IJE.2019.32.01a.08
20. Samantaray S, Dash P, Panda G. Distance relaying for transmission line using support vector machine and radial basis function neural network. International Journal of Electrical Power & Energy Systems. 2007;29(7):551-6. https://doi.org/10.1016/j.ijepes.2007.01.007
21. Jena MK, Samantaray S. Intelligent relaying scheme for series-compensated double circuit lines using phase angle of differential impedance. International Journal of Electrical Power & Energy Systems. 2015;70:17-26. https://doi.org/10.1016/j.ijepes.2015.01.035
22. Rahmkhoda E, Faiz J, Abedini M. Detection of loss-of-excitation in synchronous machines using hybrid GMDH neural network intelligent algorithm in the presence of UPFC in power system. Electric Power Components and Systems. 2023;51(10):972-90. https://doi.org/10.1080/15325008.2023.2187096
23. Rahmkhoda E, Faiz J, Abedini M. Detecting loss of excitation condition of synchronous generator in the presence of unified power flow controller based on data mining method. Electric Power Systems Research. 2024;228:109975. https://doi.org/10.1016/j.epsr.2023.109975
24. Silva H, Coelho A, Faria I, Araujo B. ANN based impedance trajectory detection approach for loss of excitation protection of synchronous generators connected to transmission lines with SVCs. Electric Power Systems Research. 2022;213:108766. https://doi.org/10.1016/j.epsr.2022.108766
25. Gulati V, Verma K, editors. Supervised Machine Learning to Identify Loss of Excitation and Power Swing in a Generator. 2023 7th International Conference on Computer Applications in Electrical Engineering-Recent Advances (CERA); 2023: IEEE. 10.1109/CERA59325.2023.10455561
26. Ramadoss H, Muthiah G. Ensemble machine learning approach to identify excitation failure in synchronous generators. Engineering Failure Analysis. 2023;152:107506. https://doi.org/10.1016/j.engfailanal.2023.107506
27. Noori H, Yaghobi H. A Protection for Loss of Field in Synchronous Generator in Presence of Series Compensation Capacitor. International Journal of Engineering Transactions C: Aspects. 2024;37(9):1857-67. https://doi.org/10.5829/IJE.2024.37.09C.15
28. Zoghi M, Yaghobi H. Synchronous generator dual estimation using sigma points Kalman filter. International Journal of Engineering Transactions A: Basics. 2024;37(07):1239. https://doi.org/10.5829/ije.2024.37.07a.04
29. H. A-A. Reduce harmonic orders of voltage waveform in the synchronous generator by changing the winding structure. International Journal of Engineering Transactions B: Applications. 2025;38(8):2008-17. https://doi.org/10.5829/ije.2025.38.08b.22
30. Berdy J. Loss of excitation protection for modern synchronous generators. IEEE Transactions on Power Apparatus and systems. 2006;94(5):1457-63. https://doi.org/10.1109/T-PAS.1975.31987
31. Hasani A, Haghjoo F. A secure and setting-free technique to detect loss of field in synchronous generators. IEEE Transactions on Energy Conversion. 2017;32(4):1512-22. https://doi.org/10.1109/TEC.2017.2697501
32. Marchi P, Estevez PG, Messina F, Galarza CG. Loss of excitation detection in synchronous generators based on dynamic state estimation. IEEE Transactions on Energy Conversion. 2020;35(3):1606-16. https://doi.org/10.1109/TEC.2020.2985529
33. Momeni E, Yaghobi H, Shahzadi A. Using dynamic state estimation to detect loss of excitation in synchronous generators. IET Generation, Transmission & Distribution. 2024;18(3):639-52. https://doi.org/10.1049/gtd2.13106
34. Sauer PW, Pai MA, Chow JH. Power system dynamics and stability: with synchrophasor measurement and power system toolbox: John Wiley & Sons; 2017.
35. Yaghobi H. Fast discrimination of stable power swing with synchronous generator loss of excitation. IET Generation, Transmission & Distribution. 2016;10(7):1682-90. https://doi.org/10.1049/iet-gtd.2015.1045
36. Goldsworthy DL. A linearized model for MOV-protected series capacitors. IEEE Transactions on Power Systems. 2007;2(4):953-7. https://doi.org/10.1109/TPWRS.1987.4335284
37. Marttila R. Performance of distance relay mho elements on MOV-protected series-compensated transmission lines. IEEE transactions on power delivery. 2002;7(3):1167-78. https://doi.org/10.1109/61.141827
38. Yaghobi H. Real-Time Discrimination of Symmetrical Faults from Power Swings. Iranian Journal of Electrical & Electronic Engineering. 2023;19(2). https://doi.org/10.22068/IJEEE.19.2.2658
39. Yaghobi H. Out-of-step protection of generator using analysis of angular velocity and acceleration data measured from magnetic flux. Electric Power Systems Research. 2016;132:9-21. http://dx.doi.org/10.1016/j.epsr.2015.11.003
40. Edition S. The authoritative dictionary of ieee standards terms. IEEE Std. 2000:100-2000. https://doi.org/10.1109/IEEESTD.2000.322230

APPENDIX

TABLE 2. The Network Studied Parameters

Generator		
S= 390 MVA, V=13.8 kV, f= 60 Hz, H= 5.5 s		
$X_d(pu)=1.305,\ X'_d(pu)=0.296,\ X''_d(pu)=0.252,$		
$X_q(pu)=0.474,\ X'_q(pu)=0.2,\ X''_q(pu)=0.243,$		
$T'_{do}(s)=5,\ T''_{do}(s)=0.1,\ T'_{qo}(s)=0.8,\ T''_{qo}(s)=0.09,$		
$X_l(pu)=0.18,\ R_s(pu)=0.0016$		
LOF Relay		
Original setting: Z_1=1 p.u., Z_2=1.305 p.u., Reduced setting: Z1=0.323 p.u., Z2= 0.4215 p.u., Time delay for Z1 =0.1 s, Time delay for Z2= 0.5 s, UV element=0.87 p.u. with 1 s time delay, R_C=1600, R_V=200.		
Transformer	**Series compensation module**	**Line**
S= 475 MVA, 13.8/400 kV, $R_1(pu)=0$, $L_1(pu)=0.15$, $R_2(pu)=0$, $L_2(pu)=0.15$	Total line reactance in positive seq. (x_1) =$w\times l_1$ *(H/km)* × Line length (km) Series compensation capacitor reactance (X_c) =$x_1\times k$ (Degree of Comp.) **MOV** Reference current=30 kA Total Capacitor full load current (I_{cn})=2 kA , $I_{pr}=2.5\times I_{cn}$, Reference voltage=sqrt (2)× X_c × I_{pr}	Length (km)=300, r_1(ohms/km)=0.01273, r_0(ohms/km)=0.3864, l_1(H/km)=0.9337e-3, l_0(H/km)=4.1264e-3, c_1(F/km)=12.74e-9, c_0(F/km)=7.751e-9

TABLE 3. Parameters of the Utilized Hydraulic Turbine and AVR

Hydraulic turbine & PID	AVR
Servo-motor: $k_a(pu)=3.33, T_a(s)=0.07$	Low-pass filter: $T_r(s)=20e-3$
Droop: $R_p(pu)=0.05$	Regulator: $k_a(pu)=300, T_a(s)=0.001$
Regulator: $k_p=1.163, k_i=0.105,$ $k_d=0, T_d(s)=0.01$	Damping filter: $k_f(pu)=0.001, T_f(s)=0.1$
Hydraulic turbine: $\beta=0, T_w(s)=2.67$	Exciter: $k_e(pu)=1, T_e(s)=0$
Gate opening limits: $g_{\min}(p.u)=0.01, V_{g\min}(p.u/s)=-0.1$ $g_{\max}(p.u)=0.975, V_{g\max}(p.u/s)=0.1$	Output Limits: $V_{f\max}(p.u)=11.5,$ $V_{f\min}(p.u)=-11.5$

Persian Abstract

چکیده

تشخیص خطای قطع تحریک ژنراتورهای سنکرون در شبکه‌های قدرت جبران‌شده با خازن‌های سری محدودیت‌هایی دارد. هنگامی که جریان‌های خطا از بانک خازنی سری عبور می‌کنند، اضافه ولتاژهایی ایجاد می‌شوند که از مقادیر نامی بانک های خازنی تجاوز می‌کنند. بنابراین، بانک های خازنی در برابر جریان‌های خطا، معمولاً توسط یک مقاومت غیرخطی به نام وریستور اکسید فلزی محافظت می‌شوند. از سوی دیگر، هنگامی که بانک خازنی و مقاومت غیرخطی آن در حلقه امپدانس خطا قرار می‌گیرند، شرایط برای رله قطع تحریک در محل ژنراتور نامطلوب می‌شود. این شرایط نامطلوب شامل پدیده‌های زیادی مانند تغییرات جریان و/یا ولتاژ، نوسانات فرکانس بالای ناشی از مقاومت های غیرخطی و نوسانات زیرسنکرون است. بنابراین، در این تحقیق یک شاخص جدید مبتنی بر امپدانس اصلاح‌شده، برای حفاظت قطع تحریک یک ژنراتور سنکرون در حضور خازن سری و تجهیزات اضافه ولتاژ مرتبط با آن ارائه می‌دهد. در این تحقیق از رله قطع تحریک Berdy استفاده شده است. همچنین از نرم‌افزار "Matlab/Simulink" برای شبیه‌سازی حوزه زمان خازن سری و تجهیزات اضافه ولتاژ آن استفاده شده است. با شبیه‌سازی سناریوهای مختلف، اثربخشی و عملکرد رضایت‌بخش تکنیک اصلاح‌شده پیشنهادی و استقلال آن از ساختار سیستم قدرت نمایش داده شده است.